Environmental Science Nano

Accepted Manuscript

ROYAL SOCIETY OF CHEMISTRY

rsc.li/es-nano

Environmental Science: Nano RSCPublishing

ARTICLE

Microwave-assisted incorporation of silver nanoparticles in paper for point-of-use water purification

www.rsc.org/

Theresa A. Dankovich[a, b]

This work reports an environmentally benign method for the *in situ* preparation of silver nanoparticles (AgNPs) in paper using microwave irradiation. Through thermal evaporation, microwave heating with an excess of glucose relative to the silver ion precursor yields nanoparticles on the surface of cellulose fibers within three minutes. Paper sheets were characterized by electron microscopy, UV-Visible reflectance spectroscopy, and atomic absorption spectroscopy. Antibacterial activity and silver release from the AgNP sheets were assessed for model *Escherichia coli* and *Enterococci faecalis* bacteria in deionized water and in suspensions that also contained with various influent solution chemistries, i.e. with natural organic matter, salts, and proteins. The paper sheets containing silver nanoparticles were effective in inactivating the test bacteria as they passed through the paper.

Introduction

Due to inadequate water and sanitation services in many parts of the world, 780 million people do not have access to clean, potable water sources.[1] This has caused the spread of preventable water-borne diseases by microbial contaminants, such as giardiasis, cholera, cryptosporidiosis, gastroenteritis, etc.[1] One of the possible solutions to reducing the microbial contamination of drinking water is small-scale or point-of-use (POU) systems for water treatment. POU systems are not connected to a central network, have low energy inputs, and can be used in emergency response following disasters. Functional nanomaterials, such as AgNPs, copper nanoparticles, carbon nanotubes, titania nanoparticles, have been suggested for POU treatment.[2-9] Recently, for POU applications, we have designed a paper sheet embedded with silver nanoparticles to purify drinking water contaminated with bacteria.[2]

Integration of green and sustainable processes into nanomaterial synthesis has attracted interest.[10-15] Key efforts aim to use renewable resources, nontoxic chemicals, and environmentally benign solvents, and to minimize waste generation. Generally, the deposition of metal nanoparticles on surfaces involves using strong reducing agents, and/or physical methods, such as UV irradiation and conventional thermal heat.[2,16-18] These highly reactive reducing agents, such as $NaBH_4$ and hydrazine, are not environmentally benign choices. There is growing interest in using nontoxic reducing agents, such as amino acids and reducing sugars, for nanoparticle synthesis.[10-15] Metal nanoparticles in solid matrices have potential applications as catalytic, antimicrobial, sensor, and electronic materials. Paper, as a solid matrix, is an attractive material due to its high porosity, mechanical strength, high absorbency, and natural abundance.

Microwave irradiation is emerging as a rapid and green method of heating for nanoparticle synthesis.[11,17] Microwave heating methods have been shown to increase reaction rates and product yields, compared to conventional thermal heating, due to more uniform heating of the sample.[18] Microwave irradiation has been used to synthesis nanoparticles in solution, but not extensively in solids matrices. *In situ* reduction of nanoparticles in the paper directly in the microwave oven greatly simplifies the experimental design, reduces energy inputs, and minimizes waste. In cellulosic materials, there have been a few reports of physical reduction of metals by thermal treatment.[19-21] However, to achieve uniform nanoparticles by heating, long reaction times are required, and microwave-assisted

synthesis could drastically reduce these reaction times. Cellulose-silver nanocomposites have also been prepared in regenerated cellulose via microwave-assisted synthesis.[22-24]

Typically, the main use for materials containing silver nanoparticles are antimicrobial applications, such as water filtration, wound care, food packaging, textiles, and so on. To assess the antibacterial effectiveness of AgNP papers in such applications, some of the potentially interfering chemicals were modeled in the laboratory. Model contaminants were selected from environmental and biological media, such as natural organic matter, salts, and proteinaceous materials. With other filter media, such as ceramic water filters, the relevance of understanding the interactions between dissolved substances in water sources and nanoparticle is gaining attention.[26]

Here I report the use of glucose as a reducing sugar in combination with a domestic microwave to rapidly form silver nanoparticles in paper. This method is essentially a modified version of Tollen's reaction, where ammoniacal silver nitrate is reduced by aldehydes, such as glucose, to produce metallic silver.[27] The main drawback of Tollen's reaction is the short lifetime of ammoniacal silver nitrate to decomposition to highly explosive silver nitride. Our method differs by eliminating potentially dangerous byproducts through the use of glucose and microwave heating to reduce silver nitrate to silver nanoparticles directly on the paper fiber surfaces. This work also represents an safer alternative to our previous AgNP synthesis method on paper fibers, which reduced silver ions through the strong reductant and irritant, sodium borohydride, $NaBH_4$.[2]

Following the AgNP formation and material characterization, antibacterial filtration tests were performed with the AgNP papers. We examined the impact of fulvic acid, salt, and biological nutrient media on the inactivation of *E. coli* bacteria. The various test solutions were combined with bacterial suspensions and passed through the AgNP paper sheet in a simple flow percolation experiment, as previously described.[2]

Materials and Methods

Materials

Absorbent blotting papers made from bleached softwood kraft pulp (Domtar Inc. and supplied by FP Innovations, Pointe-Claire, QC, Cosmos Blotters by Legion Paper, NY, Ahlstrom, Filtration, Mount Holly Springs, PA, and Neenah Paper, Neenah, WI), cotton fiber papers (supplied by Whatman, GE Healthcare Life Sciences, Piscataway, NJ and Ahlstrom, Filtration, Mount Holly Springs, PA), and cotton linter pulp (supplied by GP Cellulose, Memphis, TN) were used in this study. The sheet thickness and grammage for the various paper sheets are summarized in Table S1, and they are free from sizing agents, fluorescent agents and chemical additives. Nearly all the characterization and bactericidal testing was performed using the Domtar blotting paper, unless otherwise noted. Silver nitrate ($AgNO_3$), β-D-glucose, 30% hydrogen peroxide (H_2O_2), concentrated nitric acid (HNO_3), and poly(L-lysine) (0.01% solution) were purchased from Sigma Aldrich and used as received. Nutrient broth media (Luria Bertani and Lauryl Sulfate broths), tryptone, yeast extract, B-D glucose, phosphate buffered saline (PBS), and Endo agar were purchased from VWR and used as received. Fulvic acid was purchased from International Humic Substances Society (IHSS), St. Paul, MN. The fulvic acid powder was dissolved into deionized water and stirred until dissolved, approximately an hour. The concentrated fulvic acid stock solution was stored at 4°C in the dark until use. All solutions with the exception of fulvic acid were autoclaved prior to use. During the experiments, the diluted fulvic acid solution was not protected from light exposure. Phosphate buffered saline (PBS), sodium chloride, tryptone, and Luria Bertani (LB) broth are frequently used in bacteria nutrient media, and representative of concentrations encountered in biological applications. Water treated with a Barnstead Nanopure system was used throughout.

Preparation of silver nanoparticle paper

Sheets of blotting paper (10 cm by 10 cm) were immersed in freshly prepared aqueous solutions of glucose (0 to 1.0 M) and silver nitrate (0 to 0.1 M) for 10 minutes. No apparent reaction was observed at room temperature. For nanoparticle formation through thermal evaporation, the papers were either placed upright in a 400 mL glass beaker in a domestic microwave (Sharp Model No. R-410CWC, 2.45 GHz, 1000W) for 3-7 minutes or in a conventional oven at 105°C for 30-70 minutes. To avoid local overheating in the microwave oven (indicated by turning brown at hot spots due to caramelization of the glucose), the sheets were placed to avoid the hot spots, and the microwave was stopped every 30 sec. to rotate the sheets by 90 degrees around the vertical. After heating, the AgNP papers were soaked in water for 1-2 hours to remove excess unreacted reagents. For comparison, AgNP papers were also prepared by reduction with sodium borohydride.[2] Following the paper soaking step, the papers were dried in a modified plastic food container with a clamp lock to restrain the paper in order to prevent sheet curling. Parts of the top and sides of the container were removed to maximize air drying. The initially wet sheet was placed across the top of the container and clamped in place with the container lid. The dried sheet was trimmed to 6.5 cm by 6.5 cm.

Due to the possibility of the papers overheating in the microwave oven, several important and simple experimental modifications are necessary. Firstly, the careful placement of papers in the microwave by avoidance of the hot spots while heating in the microwave reduces the occurrence of side reactions of the glucose, i.e. caramelization as evidenced by brown staining. Secondly, if the papers are placed in or partially in a hot spot, the 90° rotation of the papers every 30 seconds reduces the overheating.

Characterization

Paper samples were imaged through standard photography and dark field microscopy (Hirox KH 7700). Qualitatively, color changes from white to yellow and/or orange indicate the presence of silver nanoparticles. Additionally, the presence of AgNPs in the blotting paper was confirmed by measuring the reflectance spectra of the AgNP papers with a diffuse reflectance attachment (Labosphere, DRA-CA-30) on a UV-Vis spectrophotometer (Varian TCA-Cary 300) at wavelengths of 300 to 800 nm. Reflectance was measured relative to a poly(tetrafluoroethylene) powder standard.

The shape and size distribution of the silver nanoparticles in the sheet were examined by electron microscopy. Individual paper fibers containing silver nanoparticles from the AgNP sheets were pulled from the papers and deposited on carbon coated copper grids that had been treated with poly(L-lysine), and imaged with a Philips CM200 200 kV transmission electron microscope (TEM). Nanoparticle diameters were measured for greater than 100 particles per sample, with standard deviations reported. Imaging and analysis of the AgNP paper was performed with a field emission scanning electron microscopy (Hitachi S-4700 FE- SEM) attached to an energy-dispersive X-ray spectroscopy detector (EDX). For SEM, samples were sputter coated with a thin, 24 nm, layer of AuPd prior to imaging. Image analysis was performed with GIMP 2.8.

To quantify the amount of silver in the AgNP papers, we performed an acid digestion of the paper and analyzed the amount of dissolved silver with a flame atomic absorption (FAA) spectrometer (Perkin Elmer AAnalyst 100) as described previously.[2] The silver content reported is five replicates per sample concentration with standard error reported. To analyze for the deposition of glucose oxidation products on the AgNP sheets, we used the following methods. First, we evaluated the weight difference before and after nanoparticle formation. Second, we soaked the paper sheets in water for 120 minutes to remove the sugars and analyzed the aqueous extracts for reaction byproducts with a UV-Vis spectrophotometer. Absorbance at 280 nm corresponds to conjugated carbonyl intermediate byproducts from caramelization reactions.[28]

Bactericidal testing

The AgNP papers were evaluated for bactericidal effectiveness by a simple water filter test, as previously detailed.[2] Nonpathogenic *Escherichia coli* and *Enterococci faecalis* bacteria, which are indicators of faecal contamination, were used as the test bacteria. Suspensions of lab-cultured bacteria in deionized water were separately passed through a 6.5 cm by 6.5 cm square paper, and the bacteria was separated from the effluent water, to prevent prolonged exposure to dissolved silver. The bacteria pellet was re-suspended in deionized water and analyzed for viable bacteria by plating on nutrient agar plates and incubating at 37°C for 24 hours. As controls, we also filtered the bacteria through an untreated and glucose saturated paper sheets. In some tests, the bactericidal activity was evaluated against a nonpathogenic wild strain of *E. coli*, which was obtained from IDEXX (IDEXX Laboratories, Inc., Maine). A bacteria suspension of $5x10^4$ or $4x10^9$ colony-forming units (CFU)/mL of *E. coli* was passed through a 6.5 cm by 6.5 cm square or a 20 cm circular paper (Figure 1). The effluent water was tested for live bacteria by shaking 100 mL of effluent water with an IDEXX Colilert pack and subsequent sealing in IDEXX Quanti-Tray 2000. The IDEXX trays were incubated overnight at 37°C for 24h and the positive wells were counted[29]. Unless noted, all bactericidal tests were performed by water passage through the square filter holder.

FIGURE 1. Images of different shapes and sizes of the AgNP Domtar paper: a) 42.25 cm^2 square and b) 314 cm^2 circle (both with a thickness of 0.5 mm). Filter holders for the AgNP papers include: c) square unit and d) plastic sieve inserted into bucket.

In addition, antibacterial stress-tests were performed, where the composition of the influent water was varied to include high levels of model contaminants, such as natural organic matter (fulvic acid), sodium chloride, and biological growth media (tryptone and LB broth). In these experiments, only *E. coli* bacteria were evaluated. To ensure a well dispersed bacterial suspension in these various feed solutions, the suspensions were thoroughly mixed with a vortex mixer prior to filtration. Five replicates were performed per paper, and the standard error was reported.

Silver release and retention

Following the bactericidal testing, the effluent water was centrifuged to separate the bacteria from the supernatant. Both the supernatant and bacterial pellet were analyzed for silver by graphite furnace atomic absorption spectrometry (GF-AA, Perkin Elmer AAnalyst 100), as described previously.[2] The bacterial pellet was digested prior to analysis as described following a previously published method.[2] Five replicates were performed per paper, and the standard error was reported. The percent silver retention was determined from the silver release subtracted from the overall silver content of the paper.

After passing through the AgNP paper, the effluent water was also analyzed for the presence of silver nanoparticles by UV/Visible spectrophotometry (TCA - Cary 300, Varian). The spectrophotometric method qualitatively detects silver nanoparticles by the presence of a surface plasmon resonance peak around 390-420nm.[30]

Results and discussion

Paper characterization

The silver nanoparticles were readily formed in cellulosic blotter papers by both microwave irradiation

(MW) and conventional oven heating of the papers saturated with silver nitrate solution. Higher concentrations of glucose gave more uniform and smaller nanoparticles, and shortened the reaction times in both the microwave and conventional oven (Table 1). The chemical reaction for this synthesis is as follows:

$$Ag^{+}(aq) + C_5H_{11}O_5\text{–}CHO\ (aq) + 2OH^{-} \rightarrow Ag\text{-}NP\ (s) + C_5H_{11}O_5\text{–}COOH\ (aq) + H_2O\ (l)$$

First, silver nitrate solution is absorbed onto the cellulose fibers, followed by a reduction of absorbed silver to metallic silver and an oxidation of glucose to gluconic acid. This reaction does not occur at room temperature, unless catalyzed by UV light, and typically occurs more quickly with higher temperatures. The reduction of silver nitrate to metal nanoparticles occurred during the drying of the solution-soaked paper sheets and resulted in fibers coated with silver nanoparticles.

Heating method	Reducer	Concentration (M)	Synthesis time* (min)	Nanoparticle Diameter (nm)
Microwave	none	n/a	20	13.4 ± 10.2
Microwave	Glucose	0.01	9	7.1 ± 3.2
Microwave	Glucose	0.1	5	7.2 ± 2.6
Microwave	Glucose	1	3	3.2 ± 1.6
Oven	none	n/a	8 days	5.5 ±2
Oven	Glucose	0.01	90	7.1 ±3
Oven	Glucose	0.1	75	6.9 ± 4.8
Oven	Glucose	1	40	7.5 ± 2.2
n/a	$NaBH_4$**	0.26	15	7.1 ±3.7

TABLE 1. Comparison of various methods to incorporate silver nanoparticles into the Domtar blotting paper sheets.

*Time required to generate overall yellow/orange color on the paper, if heated longer, the paper turns red and/or brown colored.

** Results from Dankovich and Gray, 2011.[2]

The sheets changed color from white to yellow/orange/brown with increasing precursor silver ion and glucose concentrations (Figure 2). The color changes in the paper sheets are due to the surface plasmon resonance (SPR) of silver nanoparticles. UV-Vis reflectance spectroscopy (Figure 2a) showed the least reflectance at 420 nm, which falls in the characteristic SPR range (390-420 nm) for a suspension of spherical silver nanoparticles.[30] The spectral broadening for the higher concentrations of AgNPs from blotting paper also is indicative of a wider size distribution than for AgNPs formed in solution and of surface effects of the paper substrate. For papers with the same precursor silver concentration, the AgNP papers formed by glucose reduction showed a slightly broader peak at 420 nm and a greater reflectance at long wavelengths (greater than 600nm) than the AgNP paper formed by sodium borohydride reduction.[2] (Figure S1). Extended heating times result in darker colored sheets from continued AgNP particle growth and byproduct formation from sugar caramelization.

FIGURE 2. Domtar blotter papers without any silver (a) untreated, (b) heated in the microwave for 30 minutes, and (c) heated in the microwave for 6 minutes with glucose. Blotter papers were heated in the microwave for 4-6 minutes with 1M glucose and the following $AgNO_3$ concentrations: (d) 1 mM (e) 10 mM (f) 25 mM, and (g) 100 mM (each sheet is 6.5 x 6.5 cm) to form silver nanoparticles in the sheets.

FIGURE 3a. UV-Visible reflectance spectra of paper sheets after being soaked with 1M glucose and increasing silver nitrate concentrations: a) 1 mM, b) 5 mM, c) 10 mM, d) 25 mM, and e) 50 mM, and then heated by microwave irradiation. 3b. UV-Visible reflectance spectra of paper sheets with different initial glucose concentrations: a) 0.01 M b) 0.1M and c) 1.0 M, and 1 mM $AgNO_3$ as the initial silver ion concentration, prepared by oven heating at 105°C for 70 minutes.

Following the microwave-assisted reduction of silver with glucose in the paper, the surface of the paper fibers was covered with small spherical nanoparticles and larger cubic nanoparticles, as shown in the SEM images (Figure 3). From TEM images, the average diameter of the spherical AgNPs was 5.5 nm with a standard deviation of 3.6 nm. (Table 1 and Figure 4). The cubic nanoparticles tended to be around 50 nm per side (Figure 3b). Generally, the electron microscopy images showed similar sizes and shapes for the nanoparticles made by both the oven and microwave heating methods. These are typical sizes for silver nanoparticles prepared *in situ* on cellulosic fibers,[1,7,14,25] although only spherical nanoparticles were observed after $NaBH_4$ reduction.[2] Samples heated in the microwave without any glucose showed a greater proportion of cubic nanoparticles and had the largest nanoparticles with an average diameter of 13.4 (±10.2) nm. Samples heated in the microwave with only glucose and no silver nitrate showed similar SEM images as untreated paper. An EDX peak at 3 keV confirmed the formation of silver nanoparticles in the papers (Figure S2).

FIGURE 4. Scanning electron microscope image of AgNP paper with 2.5 mg Ag/ g paper, formed by heating in microwave oven: (a) 35,000 x and (b) 60,000 x magnification.

FIGURE 5. Nanoparticle diameter size histogram of silver nanoparticles in blotting paper with 1M glucose concentration (black bars) and no glucose (gray bars), and heated in the microwave. Inset of TEM image of silver nanoparticles formed with glucose reduction and microwave irradiation.

The acid digestion of the AgNP papers showed silver content ranging from 0.53 to 5.3 mg Ag per gram of paper (0.05 to 0.5% weight percent) (Table 2). The increase in silver content of the paper correlates with the increase in silver ion concentration of the solution in which the papers were soaked, prior to the reduction. The maximum amount of silver ion absorption can be directly calculated from the $AgNO_3$/glucose solution uptake into the blotting paper. For example, based on the mass of the solution absorbed (assuming the density is ~1.07 g/mL for a 1M glucose solution), then the approximate weight of silver uptake can be determined, which is listed in the fourth column in Table 2. For most experimental conditions, these values are within the error of the atomic absorption measurements.

TABLE 2. Silver content in paper filters, measured by Flame Atomic Absorption Spectrometry, with increasing precursor silver ion concentration. The calculated silver absorption is based on complete uptake of all of the precursor silver ion into the cellulose papers.

Precursor Ag^+ ion concentration (mM)	Silver Content (mg Ag/g paper)		Calculated Ag absorption (mg Ag per g paper)
	Microwave	Oven (105°C)	
1	0.5 ± 0.2	0.7 ± 0.1	0.3
5	1.4 ± 0.3	1.5 ± 0.2	1.3
10	2.4 ± 0.3	2.4 ± 0.3	2.5
25	5.2 ± 0.5	5.3 ± 0.6	6.3

After drying, a significant amount of glucose also remained in the paper. For a typical experiment, the initial glucose concentration in the reagent bath was 1M, and following NP synthesis, the dried paper had a weight gain of 26%, rendering the sheets stiff and brittle. However, following soaking in water for two hours, much of the sugar was removed from the paper, as the total weight gain was 4% and the paper reverted to its initial flexibility. The water only acted to remove excess sugar, as the silver content in the AgNP papers remained the same (typically less than 1% weight percent).

Effect of glucose

Without glucose, the production of AgNP was slow, with reaction times of over 15 minutes for microwave irradiation and over several days for conventional oven heating (Table 1). The sheets with the lowest silver concentration barely showed any nanoparticle formation, and the sheets with the highest silver concentration appeared non-homogeneous with larger, agglomerated particles in some areas and only a few nanoparticles in other spots. These non-homogeneous sheets had variegated coloration with purple, red, orange, and yellow regions. The red shift in UV-Vis absorbance for AgNP nanoparticles corresponds to an increase in particle aggregation and size. This results from a uncontrolled irregular AgNP formation.

The addition of glucose greatly sped up the reaction and led to a more predictable synthesis. As the glucose concentration was increased from 0.01 to 1.0 M, the nanoparticle formation time decreased and less particle aggregation was observed. The reflectance spectra from UV-Vis measurements showed a deeper orange color with higher glucose concentrations (Figure 2b). The average nanoparticle diameter decreased from 7.2 nm for 0.01 M glucose to 3.2 nm for 1 M glucose (Table 1). Higher concentrations of glucose appeared to facilitate the nucleation of silver nanoparticles. The microwave-assisted formation of silver nanoparticles occurred in 3-7 minutes with a glucose concentration of 1.0 M. Similar trends were observed with oven heating, but the overall reactions were much slower. Additionally, similar trends of a higher ratio of reducing agent to silver ion concentrations resulted in more uniform nanoparticle synthesis was also observed with sodium borohydride reduction.[2,31] Even though the AgNP formation reaction occurs via a stoichiometric ratio, the excess reducing agent is necessary to prevent silver nanoparticle aggregation.

Effect of heat source

The quicker AgNP formation in microwave synthesis is most likely due to the much quicker water evaporation, as the frequency of domestic microwaves of 2.45 GHz is optimized for the absorption of energy into water. This evaporation occurs at just below the boiling point of water, which corresponds to the oven temperature used in this study. If higher oven temperatures were used, presumably faster water evaporation would occur and therefore faster AgNP formation. However, the cellulose polymer begins to degrade at temperatures greater than 150°C[32], and AgNP formation at elevated temperatures would lead to a weaker

structure for the paper filter, which would shorten its lifespan as a water filter.

The elevated reaction temperature solely appears responsible for the formation of cubic shaped silver nanoparticles, as cubic particles were observed in silver nitrate soaked paper samples heated without glucose. The TEM and SEM images (Figures 3, 4) suggest that the AgNP paper sheets have a mixture of spherical and cubic nanoparticles, which could be attributed to the smaller spherical particles forming quickly due to the reducing sugar and larger cubic particles more slowly forming due the heat source. In contrast, the sodium borohydride synthesis, which is typically used to produce "seed" nanoparticles, did not result in any cubic particle formation.[2] Other studies have shown an increasing proportion of silver nano-cubes to spherical AgNPs with higher synthesis temperature.[33-34]

As discussed earlier, the domestic microwave heating was inhomogeneous due to the formation of standing waves, which result in some spots overheating, so called "hot spots". If heated in a hot spot in the microwave, a paper sheet saturated with an aqueous glucose solution (1M) resulted in the formation of browning due to caramelization. In contrast, no discoloration or signs of caramelization were observed when a similar glucose-saturated sheet was heated in a conventional oven or the sheet was periodically rotated in the microwave during heating. The microwave hot spots can cause significant elevation in temperature to much higher than 100°C, the boiling temperature of water, as the domestic microwave is optimized for. For example, glucose only undergoes complex caramelization reactions at temperatures greater than 160°C, resulting in hundreds of chemical products, including furans, furanones, pyrones, and carbocyclics.[35-36]

To prevent excessive heating in the microwave, the samples were periodically rotated every thirty seconds for the duration of AgNP formation. To monitor the formation of caramel byproducts, UV-Vis spectroscopy was used to measure the spectra of aqueous extracts from AgNP paper sheets for the presence of caramel byproducts. These byproducts include 5-(hydroxymethyl)furfural (HMF), which is detected in the range 270-300 nm, and the kinetics of caramelization can be monitored by the measurement of HMF concentration.[28,35] Overall, the microwave-heated samples showed minor spectral variations due to spots overheating in the microwave (Figure S3). The browning from microwave hot spots showed the greatest absorbance in the 270-300 nm range, as would be expected (Figure S3). The samples heated in the conventional oven did not show any spectrophotometric evidence of caramelization. Compared with the silver content in non-caramelized AgNP papers, the silver content of the brown caramel spots was 30% reduced. This suggests that caramelization is acting as a competing reaction. With periodic rotation to prevent excessive heating, even if the paper was briefly placed in a hot spot in the microwave oven, the detection of formation of caramel byproducts was not observed as evidenced by the near zero absorbance at 280 nm (Figure S4). If the paper was not placed in a hot spot in the microwave, then no caramelization was observed, and only silver nanoparticle synthesis occurred. Care should be taken experimentally to avoid overheating of the papers during AgNP formation. In all subsequent analyses, all AgNP papers that were heated in the microwave were periodically rotated during the heat treatment.

The influence of paper chemistry

The majority of the experiments presented in this study focused on a singular model of a wood pulp paper without any chemical additives (Domtar blotting paper). This has served as an excellent starting point to explore other paper choices, which differ by fiber type and coatings and additives on the cellulose fibers. As for this method for silver nanoparticle formation on paper fibers, there were noticeable differences with the fiber type and the paper coatings. Fifteen different papers were tested for this AgNP formation method (Table S1), where some differences in silver absorption and nanoparticle formation were observed. When the papers were characterized by fiber type, it was clear that papers made from wood pulp fibers had greater than two times more AgNP formation with the same starting conditions (10 mM $AgNO_3$ and 1M glucose) (Table S1). The silver nanoparticle content of 3.6 mg Ag per g paper in the wood pulp cellulose papers, while the cotton cellulosic papers averaged around 1.5 mg Ag per g paper. Two particular differences that may increase the silver uptake into the wood pulp fibers include a lower percentage of crystalline ordered regions[37] and a higher content of carboxylic acid groups in wood pulp than cotton[38]. For greater silver absorption into cellulose and other fibers, other researchers have used various oxidative surface treatments to increase carboxylic acid groups[18], polyelectrolyte multi-layering[39], and nano-fibers with higher surface area[18,31].

Various coatings on cellulosic fibers can complicate this AgNP formation method. Hydrophobic coatings prevent the absorption of silver nitrate into the fibers, and as a result, no reaction occurs. Sizing agents can react with silver nitrate at room temperature and lead to irregularly large-sized AgNPs on the fibers and AgNP formation in the soak solution. The best paper choice has a high degree of water absorption and is free from additives.

Antibacterial activity

The antibacterial activity of sheets prepared by both microwave and conventional heating was measured, as described previously.[2] To assess the bactericidal effectiveness of AgNP paper, we added the isolated effluent bacteria, after passage through the paper, to nutrient agar plates. The plate count experiments showed log 8.1 and log 2.3 reductions of viable *E. coli* and *E. faecalis* bacteria, respectively, in the effluent, as compared to the initial concentration of bacteria ($1x10^9$ CFU/mL for *E. coli* and $2x10^8$ CFU/mL for *E. faecalis*) (Figure 6). This is

significantly higher than the physical filtration due to the paper alone, as the untreated papers only retained around 1.0 log of each type of bacteria. Following bacteria filtration, the AgNP papers appeared unaltered via SEM imaging and no presence of bacteria on the papers was noticeable. The paper prepared by soaking in only glucose solutions did not show any difference from the control sample for the reduction in bacteria count, with a log reduction of 0.5 and a log increase of 0.2, for *E. coli* and *E. faecalis*, respectively. Caramelization byproducts do not show any synergistic effects with AgNPs, and some intermediates, such as furfural and HMF, have been suggested to be used as an alternative growth media source for enteric bacteria.[40]

FIGURE 6. Log reduction of *E. coli* (a), (c), and *E. faecalis* (b), (d), bacterial count after permeation through the silver nanoparticle paper, at different silver contents in paper. (a) and (b) represent AgNP papers formed via sodium borohydride reduction. (c) and (d) represent AgNP papers formed via glucose and heat reduction via both microwave and conventional oven. (There was no significant differences between heating methods, so the results are averaged.) Initial bacterial concentration, $1x10^9$ CFU/mL for *E. coli* and $2x10^8$ CFU/mL for *E. faecalis*. Error bars represent standard error.

Our hypothesis on the mechanism of this AgNP paper is that bacteria accumulate silver ions from direct contact with "bare" AgNPs in the paper, and over time become inactivated. Other researchers have shown that the inactivation of bacteria from AgNPs is dependent solely upon the release of silver ions and subsequent uptake into the cells.[7,41] The release rate of silver from AgNPs is dependent upon many factors including: dissolved oxygen, nanoparticle coatings (or lack there of in this study), and geometry of the particles.[42]

The experimental procedure separates the bacteria from the effluent water by centrifugation and removal of the supernatant, which will limit the long term exposure of bacteria to the dissolved silver in the effluent water. From this study, the precise time of bacterial inactivation is not known, as absorbed silver in the bacterial cells has the potential to cause cellular damage over the 24 hour period in the incubator. However, from other studies, it appears silver ions can rapidly inactivate bacteria from as short as 15 seconds[7,43] to a few hours[44], depending upon the environmental conditions.

Effect of filtration time on antibacterial properties

The average filtration time decreased following deposition of nanoparticles on the paper, as the AgNP papers filtered nearly twice as fast as the untreated papers (Table 3). The time to filter 0.1 L of bacterial suspensions through the plastic square filter varied from 10 to 25 minutes, with the *E. faecalis* filtered through the AgNP paper (sodium borohydride formation method) being the fastest and with *E. coli* through the untreated paper being the slowest. The processes of wetting, heating, and drying the paper sheets during AgNP formation are likely to cause changes in inter-fiber interactions and increase the void space in the filter paper. The size ratio of the nanoparticles with respect to the wood pulp paper fibers themselves is 1 to 1000, and the weight percent of AgNPs is typically very low (less than 1%), so the addition of nanoparticles to fibers would not be expected to alter the packing arrangement of the fibers. The main impact on the filtration rate was due to the AgNP formation processes, not due to the small differences in silver content. The overall filtration process was quite slow due to the small volume capacity of the square plastic filter unit (Figure 1), and was a uniform flow rate for the samples tested.

Additionally, all papers evaluated filtered *E. faecalis* suspensions significantly faster than *E. coli* suspensions (Table 3). The typical size of *E. faecalis* bacteria is ~0.5 micrometer, while *E. coli* are slightly larger; 0.5 μm by 2 μm; both of which should be able to pass through the paper without a problem. For the papers evaluated, the minimum particle retention size was not reported; a comparison between the flow rate for similar papers suggests that the particle retention is between 3 micrometers to greater than 20 micrometers (Table S1). Based on differences in filtration time, there may be greater physical retention of *E. coli* than *E. faecalis,* which also may contribute to a higher log reduction of the *E. coli.* The higher reduction of *E. coli* may also be due to the increased time exposed to the silver nanoparticles in the paper from the longer filtration time.

Paper Sample	Filter shape	Flow Rate (L/hr) Average	SE
Untreated paper	square	0.24	0.01
AgNP paper (Na borohydride)	square	0.46	0.03
AgNP paper (glucose)	square	0.35	0.02
AgNP paper (glucose)	circle	4.90	0.60
AgNP paper (glucose)	square	2.10	0.23
E. faecalis			
Untreated paper	square	0.39	0.04
AgNP paper (Na borohydride)	square	0.62	0.02
AgNP paper (glucose)	square	0.55	0.03

TABLE 3. Flow rate (Liters per hour) for various filter papers with respect to the type of bacteria filtered. All papers tested were from Domtar, unless otherwise noted. Standard error is reported.

To investigate whether increasing the flow rate and therefore decreasing the time of exposure to the silver nanoparticles affects the viability of *E.coli* bacteria, the

following aspects have been varied: area of paper and fiber packing density. To test a larger paper area, a 10 L bucket with a plastic sieve inserted into the lid was used (Figure 1). The diameter of the sieve and paper filter was 20 cm, which is 314 cm^2 compared to the filter square of 42.25 cm^2 (approximately 7 times greater area). Similarly, the flow rate through the larger paper increased by greater than 5 times faster (Table 3). This did not show a significant difference in bactericidal effectiveness between the two paper sizes (Table S2).

The fiber packing density was tested by comparing a less dense pulp sheet by GP cellulose (grade 512) to the more dense blotting paper by Domtar. As shown in the SEM and dark field microscopy images in Figure 7, the void space between the fibers is more greater for the GP cellulose sheet than the Domtar sheet. With a sheet such as the Domtar blotter, with higher fiber content and less void space between the fibers, the flow rate would be expected to be much slower through the paper than other filter papers. The water flow rate through the GP cellulose sheet was 6 times faster than the Domtar (Table S1), and the flow rate with a bacteria suspension was still 2 - 4 times faster (Table 3). This did not show a significant difference in bactericidal effectiveness between the two paper types (Table S2). In contrast to the Domtar blotters, filtration through the untreated GP cellulose pulp sheet showed negligible *E. coli* retention, less than 0.1 log reduction. The faster filtration and lesser physical filtration with the AgNP - GP Cellulosepapers, this suggests the bacterial inactivation is mostly due to the exposure to the silver nanoparticles.

FIGURE 7. Scanning electron micrographs of the fiber packing density of the (a) Domtar and (b) GP Cellulose (732 g/m^2) papers. Dark field microscopy images of (c) Domtar and (d) GP Cellulose (732 g/m^2) papers. Magnification is 150 times.

Effect of model contaminants on antibacterial properties

The impact of some model contaminants on the bactericidal effectiveness of the AgNP paper has been examined. As a model natural organic matter, fulvic acid had essentially no negative effect on the bactericidal action at both concentrations analyzed, 10 and 50 mg/L. PBS showed a slight decrease to an average 7.2 log reduction for *E. coli*. However, nutrient growth media and tryptone, as models for proteinaceous contaminants, did lower the effectiveness of the AgNP paper. With the higher proteinaceous contaminants of 10 g/L for tryptone and LB broth, similar log reduction values of 3.9 and 4.3, respectively, were observed. This detrimental effect appears to be concentration dependent: with the lower LB broth concentration (1 g/L protein) filtered through the higher silver content paper, 2.5 mg/g paper, resulted in near zero viable *E. coli* bacteria (Figure 8).

FIGURE 8. Log reduction of *E. coli* bacterial count after permeation through the silver nanoparticle paper, with different influent solutions: (a) deionized water, (b) 10 mg/L fulvic acid, (c) 50 mg/L fulvic acid, (d) phosphate buffered saline, (e) 2.5 g/L LB broth, (f) 25 g/L LB broth, and (g) 10 g/L tryptone. Initial bacterial concentration, $1x10^9$ CFU/mL for *E. coli.* Error bars represent standard error.

Silver release

The AgNP papers lost very little silver during filtration experiments, with an average value of 105 ± 36.3 µg/L in the effluent water. These values are comparable to our previously published results[2]. With the fulvic acid solutions, we observed the highest concentration of silver associated with the bacterial pellet (181 - 228 µg/L) out of all the test solutions, and a similar level of silver in the effluent water (Table 4). The LB broth and tryptone solutions presented an unexpected observation followed from the silver content analysis of effluent water and bacteria. LB broth and tryptone showed the highest silver loss in the effluent water with values of 306 µg/L and 200 µg/L, respectively, and the lowest silver content in the effluent bacteria with less than 10 µg/L (Table 4). The NaCl solutions showed a fairly low level of silver release (41 µg/L) at the lower concentration (0.59 g/L NaCl), which was much less than the silver release for deionized water (105 µg/L), and an increase in silver release with increasing NaCl concentrations to comparable levels to silver release following rinses with deionized water; this trend is quite similar to silver dissolution from AgNPs in related work[45]. For all solutions evaluated, the silver loss is highest in the first couple

Test liquid	Ag release* (µg/L)	Bacterial pellet Ag absorption (µg/L)	Percent Ag loss per L
Deionized	105	15	3.1%
10 g/L tryptone	121.6	6.7	3.3%
1 g/L tryptone	200	1.3	5.2%
5.9 g/L NaCl	132	-	3.4%
0.59 g/L NaCl	41	-	1.1%
25 g/L LB broth	306	7.2	8.1%
2.5 g/L LB broth	52	7.9	1.6%
10 mg/L Fulvic Acid	94.6	181	7.2%
50 mg/L Fulvic Acid	98.1	228	8.5%
Phosphate buffer	197	-	5.1%

* Area under the curve from the data points of volumes filtered ranging from 0.1 to 1 L.

hundred milliliters and drops to close to zero ppb in an exponential decay with increasing volume of solution filtered.

TABLE 4. Silver release from the AgNP paper (2.5 mg Ag per g paper) following the antibacterial flow tests with the test liquids.

In general, the silver loss from AgNP papers is similar to that which has been reported in the literature for fibrous substrates. Silver release from consumer products, notably socks[46,47] and other water filters containing silver nanoparticles[3,39,48] has been investigated. Overall, the release of silver in the wash water of textiles varied considerably, from 3 to 1300 ppb (1-68 ug/g) for distilled water washes.[46] The silver release during washes with surfactants and oxidizers was slightly higher, with a range of 0.3 - 377 ug/g.[47] This was ascribed to specific interactions of chloride anions from detergents with AgNPs to form insoluble AgCl, and hydrogen peroxide oxidation of AgNPs to silver ions. Other filters containing silver nanoparticles showed variable silver release, depending upon the composition of the filter material. For example, polysulfone ultrafiltration membranes impregnated with silver nanoparticles released a high value of 34 ppb silver in the filter effluent, following by a decrease in silver concentration, and resulting in a 10% mass loss of silver from the filter membrane.[48] The ceramic filters with a colloidal silver coating showed an initially high silver concentration in the effluent water of 500 ppb, and over time, this dropped to under 100 ppb.[3] Polyethersulfone membranes with multilayers containing silver nanoparticles showed an average silver release of 5 ppb, which stabilized after an initial depletion period.[39]

Due to the potential release of AgNPs into the environment, researchers have examined the interactions of natural organic matter and AgNPs to predict the fate and transport.[49-52] It is likely that the fulvic acid is being adsorbed to the bacteria surface and complexing the silver, which would explain the high amount of silver found in the effluent bacteria following percolation. TEM images have shown the association of humic acids with AgNPs on the surface of bacteria,[50-51] but there are conflicting results for the bactericidal effects of this association in the literature. Fabrega et al. demonstrated less bactericidal activity of *Pseudomonas fluorescens* with higher humic acid concentrations due to a physical barrier limiting silver ion release.[50] Diagne et al. showed that humic acid had no detrimental effect on biocidal properties of AgNPs embedded in a membrane, which may be due to nanoAg being fixed to a surface instead of in suspension.[39] Dasari et al. showed a greater log reduction in mixed aquatic bacterial assemblages with humic acids in the light compared to the dark.[51] These authors attribute the difference between light and dark conditions to the reactive oxygen species formation from the humic acid,[50] which possibly occurred with our experimental conditions as no precautions were taken to prevent light exposure. The IHSS reports that the standard fulvic acid used in this study has no detectable amino acids containing sulfur groups (cysteine or methionine).[53] Although other work suggests that NOM generally contains sufficient S(II-) to have ambient Ag(I) bound as either an Ag-thiolate or as an Ag-metal sulifde complex associated with the NOM.[54] Higher concentrations of NOM slowed the silver ion release rate from AgNPs in suspensions.[42]

Following the filtration tests with LB broth, the effluent water became a faint yellow color, which is characteristic for AgNPs in suspension. To determine which broth component contributed to the AgNP release, the LB broth was separated into its major components: tryptone, a protein digest, sodium chloride, and yeast extract. Next, the various broth components at the same concentrations as in the LB broth (without bacteria) were passed through the AgNP paper and the effluent water was analyzed for the presence of silver nanoparticles by UV-Vis spectrophotometry. With LB broth and tryptone media, the presence of silver nanoparticles in the effluent water was shown by a small characteristic peak at 405-410 nm in the UV-Vis spectrum (Figure S5). The SPR peak from the tryptone was rather poorly formed and only the combination of tryptone and NaCl showed the same characteristic SPR peak for AgNPs as the LB broth did. In contrast, the NaCl rinse alone did not show any peaks in the UV-Vis spectrum, nor did the rinses with PBS, yeast extract, or fulvic acid. Based on the NaCl concentrations evaluated, the silver species in the effluent water is most likely solid AgCl,[45] which would not be expected to show any UV-Vis absorption. The combination of tryptone and NaCl in a rinse solution appears to behave somewhat differently, and suggests that the tryptone protein may complicate the typical solid AgCl formation expected at these NaCl concentrations. The very low silver absorption by the bacteria pellet and the reduced bactericidal effectiveness with the LB broth and tryptone solutions suggest that these protein-containing solutions are limiting silver ion release to the bacteria. The presence of chloride ions from the NaCl and LB broth are likely to increase the removal of silver ions from the surface of silver nanoparticles, which then may interact with the tryptone to limit the silver ion release to the bacteria. Due to the high silver content in the effluent water, LB broth proteins appear to keep silver in solution. Proteins have been shown to form a coating on the surface of silver nanoparticles.[55]

The pollution of rivers and lakes with untreated sewage not only causes the increase of coliform bacteria in natural water sources, but also increases the levels of dissolved organic materials, which are composed of approximately 50% dissolved proteins.[56] The typical values for proteins found in untreated domestic sewage range from 50 to 200 mg/L, which are considerably lower by 10-100x than the model proteinaceous contaminants in our study.[56] Due to strong interactions between silver and sulfur groups in amino acids, the presence of proteins in water contaminated with raw sewage could lead to potentially negative interactions with the embedded AgNPs in this bactericidal paper filter.

Conclusions

Silver nanoparticles were deposited on paper by either microwave irradiation or conventional oven heating in combination with glucose reduction. Direct *in situ* microwave assisted reduction of nanoparticles in the paper was rapid and convenient. The nanoparticles were well dispersed and stabilized on the paper fiber surfaces. The size of the silver nanoparticles can be controlled by concentration of silver nitrate and glucose, temperature, and duration of reaction. Local overheating, i.e. "hot spots," during microwave heating of the sheets can be avoided by periodic sample rotation. The combination of microwave irradiation and glucose reduction is more benign than the reduction with $NaBH_4$ used previously. Most importantly, the resultant AgNP paper is just as effective for inactivating bacteria during percolation through the sheet as that prepared by the previous method.[2]

Despite that the AgNP papers effectively purify water contaminated with bacteria, but water contaminated with bacteria alone is unlikely to be encountered under field conditions. The effect of some model contaminants on the effectiveness of the AgNP paper has been examined. As a model natural organic matter, fulvic acid had essentially no negative effect on the bactericidal action. However, very high levels of nutrient growth media, as models for proteinaceous contaminants, did lower the effectiveness of the AgNP paper. Although, it is highly unlikely to encounter such polluted waters, some strategies to mitigate these effects include: protecting the AgNPs in the paper sheet by an appropriate pre-filter, or allowing the contaminated water to settle prior to passage through the AgNP paper. The next step forward for this project is evaluating the bactericidal performance of these AgNP papers with surface water samples in developing countries.

Acknowledgements

This work was supported by the Sentinel Bioactive Paper Network and the Fogarty International Center at the National Institutes of Health (Award Number D43TW009359). I gratefully acknowledge the laboratory support and discussions with Derek G. Gray at McGill University and James A. Smith at University of Virginia. Additionally, I acknowledge the training and use of facilities at McGill from Glenna Keating and Isabelle Richer (Flame-AA), Line Mongeon (SEM), Xue Dong Liu (TEM), and at University of Virginia from Richard White (dark field microscopy and SEM). I also thank Ruoxi Gao and Sangjin Bae for lab assistance. David Wong (FPInnovations, Pointe Claire) helped with UV-Vis Spectroscopy.

Notes and references

[a] Department of Civil and Environmental Engineering, University of Virginia. Charlottesville, VA, 22904, USA.

[b] Department of Chemistry, McGill University, Montreal, QC H3A 2A7, Canada.
theresa.dankovich@mail.mcgill.ca

† The "hot spots" where overheating occurs due to standing waves in the microwave were plotted by a simple experiment. This involved covering a large sheet of parchment paper with a layer of chocolate chips on the microwave carousel plate. The chocolate chips were heated until specific areas started to melt and then these regions, which correspond to the "hot spots," were indicated on the parchment paper. The hot spots map was used for placement of the silver soaked papers in the microwave for these experiments. These chocolate experiments were based on a WOW Lab at McGill: http://wowlab-blueprints.mcgill.ca/en/projectpage.php?id=chocolate

1. World Health Organization, WHO, 2006. Guidelines for drinking-water quality. 137.
2. T.A. Dankovich and D.G. Gray, *Environ Sci Technol,* 2011. 4**5**(5), 1992.
3. V.A. Oyanedel-Craver and J.A. Smith, *Environ Sci Technol.* 2008. **42**(3), 927.
4. P. Jain and T. Pradeep, *Biotechnol Bioeng.* 2005. **90**(1), 59.
5. A.S. Brady-Estévez, T.H. Nguyen, L. Gutierrez, and M. Elimelech, *Water Research.* 2010. **44**(13), 3773.
6. L. Ye, C.D.M. Filipe, M. Kavoosi, C.A. Haynes, R. Pelton, and M.A. Brook, *J Mater Chem*. 2009. **19**(15), 2189.
7. D.V. Quang, P.B. Sarawade, S.J. Jeon, S.H. Kim, J.-K. Kim, Y.G. Chai, and H.T. Kim, *Applied Surface Science*. 2013. **266**, 280–287.
8. S. Lin, R. Huang, Y. Cheng, J. Liu, B.L.T. Lau, and M.R. Wiesner, *Water Research*, 2013. **47**(12), 3959-3965.
9. T.A. Dankovich and J.A. Smith, Accepted in *Water Research,* 2014.
10. B. Baruwati, V. Polshettiwar, and R.S. Varma, *Green Chem.*, 2009. **11**, 926.
11. P. Raveendran, J. Fu, and S. Wallen, *Green Chem.*, 2006. **8**(1), 34.
12. A. Panacek, L. Kvitek, R. Prucek, M. Kolar, R. Vecerova, N. Pizurova, V. Sharma, T. Nevecna, and R. Zboril. *J Phys Chem B*, 2006. **110**(33), 16248.
13. S. Horikoshi, H. Abe, K. Torigoe, M. Abe, and N. Serpone, *Nanoscale*, 2010. **2**(8), 1441.
14. B. Hu, S.-B. Wang, K. Wang, M. Zhang, and S.-H. Yu, *J Phys Chem C,* 2008. **112**(30), 11169.
15. R.M. El-Shishtawy, A.M. Asiri, N.A.M. Abdelwahed, M.M. Al-Otaibi, *Cellulose,* 2011. **18**(1),75.
16. J.H. He, T. Kunitake, and A. Nakao. *Chem Mater,* 2003. **15**(23), 4401.
17. J.A. Gerbec, D. Magana, A. Washington, and G.F. Strouse, *J Am Chem Soc*, 2005. **127**(45), 15791.

18. S. Ifuku, M. Tsuji, M. Morimoto, H. Saimoto, and H. Yano, *Biomacromolecules*, 2009. **10**(9), 2714.
19. N. Kotelnikova, V. Demidov, G. Wegener, and E. Windeisen, *Russian Journal of General Chemistry*, 2003. **73**(3), 427.
20. R. Gottesman, S. Shukla, N. Perkas, L.A. Solovyov, Y. Nitzan, and A. Gedanken. *Langmuir,* 2011. **27**(2), 720..
21. J. Cai, S. Kimura, M. Wada, and S. Kuga, *Biomacromolecules,* 2009. **10**(1), 87.
22. A.R. Silva and G. Unali. *Nanotechnology,* 2011. **22**(31), 315605.
23. S.-M. Li, N. Jia, M.-G. Ma, Z. Zhang, Q.-H. Liu, and R.-C. Sun, *Carbohydrate Polymers,* 2011. **86**(2), 441.
24. S.-M. Li, N. Jia, J.-F. Zhu, M.-G. Ma, F. Xu, B. Wang, and R.-C. Sun, *Carbohydrate Polymers,* 2011. **83**(2), 422.
25. D. Breitwieser, M. M. Moghaddam, S. Spirk, M. Baghbanzadeh, T. Pivec, H. Fasl, V. Ribitsch, and C. O. Kappe, *Carbohydrate Polymers,* 2013. **94**(1), 677.
26. J. Rayner, H. Zhang, J. Schubert, P. Lennon, D. Lantagne, and V. Oyanedel-Craver, *ACS Sustainable Chem Eng,* 2013. **1**(7), 737.
27. D. Yu, and V. W.-W. Yam, *JACS*, 2004. **126**(41), 13200.
28. L.W. Kroh, *Food chemistry,* 1994. **51**(4), 373.
29. S.C. Edberg, M.J. Allen, D.B. Smith, N.J. Kriz, 1990. *Appl and Environ Microbiology,* **56**(2), 366.
30. A. Henglein, *Chem. Mater.*, 1998. **10**, 444.
31. Maneerung, T., Tokura, S., Rujiravanit, R. *Carb Polymers*, 2008, **72**(1), 43.
32. Klemm, D., Philipp, B., Heinze, T., Heinze, U., Wagenknecht, W., *Fundamental and Analytical Methods, Comprehensive Cellulose Chemistry,* 1998, **1**, 110.
33. Y.G. Sun and Y.N. Xia. *Analyst*, 2003. **128**(6) 686.
34. T. Zhao, J.-B. Fan, J. Cui, J.-H. Liu, X.-B. Xu, and M.-Q. Zhu, *Chemical Physics Letters*, 2011. **501**(4-6), 414.
35. R.S. Shallenberger and G.G. Birch, *Sugar Chemistry*. 1975, Westport, Connecticut: AVI Publishing Company, Inc.
36. K. Licht, C. Smith, and J. Mendoza, *Food and Chemical Toxicology,* 1992. **30**(5), 365.
37. H.-P. Fink, E. Walenta, *Papier,* 1994, **48**(12), 739.
38. H. Schleicher, H. Lang, *Papier* 1994, **48**(12),765.
39. F. Diagne, R. Malaisamy, V. Boddie, R. D. Holbrook, B. Eribo, and K.L. Jones. *Environ Sci Technol*. 2012. **46**(7), 4025.
40. R. Boopathy, H. Bokang, and L. Daniels, *Journal of Industrial Microbiology and Biotechnology*, 1993. **11**(3), 147.
41. Z.-M. Xiu, Q.-B. Zhang, H.L Puppala, V.L. Colvin, and P.J. Alvarez, *Nano Lett.* 2012. **12,** 4271–4275.
42. J. Liu and R.H. Hurt, *Environ Sci Technol.* 2010. **44**(6), 2169.
43. S.-L. Loo, A.G. Fane, T.-T. Lim, W.B. Krantz, Y.-N. Liang, X. Liu, X. Hu, *Envrion Sci Technol,* 2013. **47**,9363.
44. K. Chamakura, R. Perez-Ballestero, Z. Luo, J. Liu, *Colloids and Surfaces B: Biointerfaces.* 2011, **84**(1) 88.
45. C. Levard, S. Mitra, T. Yang, A.D. Jew, A.R. Badireddy, G.V. Lowry, and G.E. Brown, Jr., *Environ Sci Technol.* 2013. **47**(11), 5738.
46. T. Benn and P. Westerhoff, *Environ Sci Technol.* 2008. **42**(11), 4133.
47. L. Geranio, M. Heuberger, and B. Nowack, *Environ Sci Technol.* 2009. **43**(17), 6458.
48. K. Zodrow, L. Brunet, S. Mahendra, D. Li, A. Zhang, Q. Li and P.J.J. Alvarez, *Water Research.* 2009. **19**(15), 715.
49. N. Akaighe, R.I. MacCuspie, D.A. Navarro, D.S. Aga, S. Banerjee, M. Sohn, and V.K Sharma, *Environ Sci Technol.* 2011. **45**(9), 3895.
50. J. Fabrega, S.R. Fawcett, J.C. Renshaw, and J.R. Lead, *Environ Sci Technol.* 2009. **43**(19), 7285.
51. T.P. Dasari and H.-M. Hwang, *Science of the Total Environ.* 2010. **408**(23), 5817.
52. R.I. MacCuspie, K. Rogers, M. Patra, Z. Suo, A.J. Allen, M.N. Martin, and V.A. Hackley, *J Environ Monit.* 2011. **13**(5), 1212.
53. International Humic Substance Society, IHSS. 2011. Retrieved November 2, 2011, from http://www.humicsubstances.org/aminoacid.html.
54. H. Manolopoulos, N.H.W. Adams, M. Peplow, J.R. Kramer, and R.A. Bell, *7th Nordic Symposium on Humic Substances in Soil and Water, Kristiansand,* 1999. Norway: Adgar College.
55. S. Kittler, C. Greulich, J.S. Gebauer, J. Diendorf, L. Treuel, L. Ruiz, J.M. Gonzalez-Calbet, M. Vallet-Regi, R. Zellner, M. Köller, and M. Epple, *J Mater Chem*. 2010. **20**(3), 512.
56. Metcalf and Eddy, Wastewater Engineering. Treatment Disposal Reuse. G. Tchobanoglous and F.L. Burton, Eds. McGraw-Hill. 1991. 1820.

Nano Impact Statement

Contaminated water in many parts of the world causes the spread of preventable water-borne diseases by microbial contaminants, such as giardiasis, cholera, cryptosporidiosis, gastroenteritis, etc. Functional nanomaterials, produced via green and sustainable processes, represent an important way to minimize the hazards of nanomaterials and can be used to disinfect water contaminated with pathogenic bacteria. In this paper, we illustrate an example of a simple silver nanoparticle synthesis using only paper soaked with silver nitrate and glucose heated in a domestic microwave for 3 minutes. Silver nanoparticle papers were evaluated for their antibacterial effectiveness with different influent water characteristics modeling natural water sources spiked with E. coli. The synthesis is novel and environmentally safe, and performs just as well as its non-sustainable synthetic counterpart. Its proposed application of a point-of-use water purifier has great potential for cleaning water in the developing world.

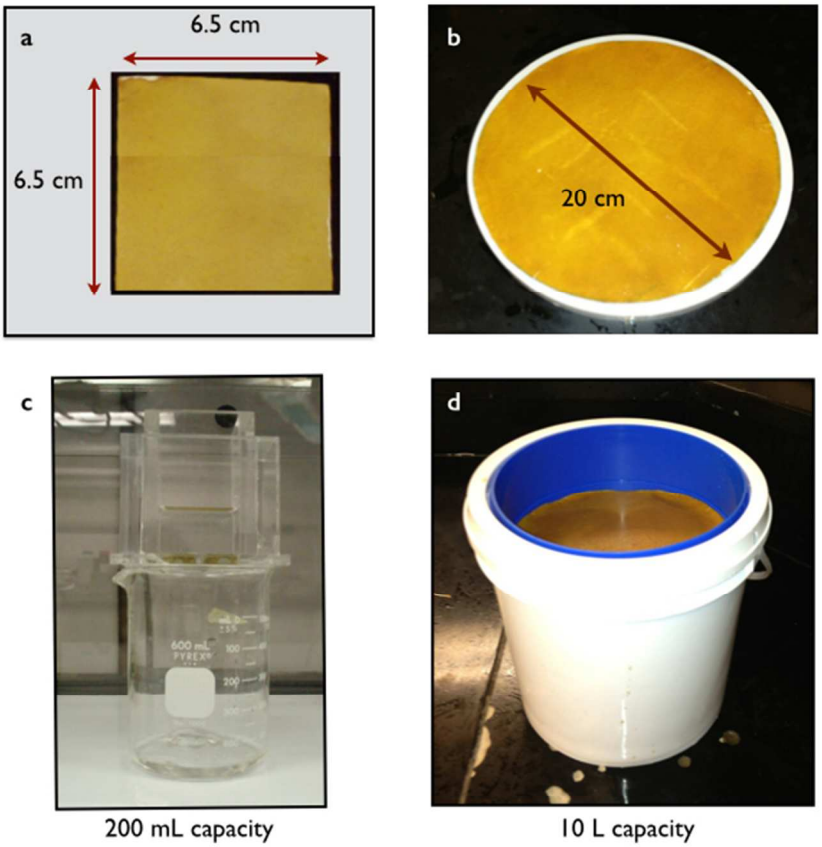

FIGURE 1. Images of different shapes and sizes of the AgNP Domtar paper: a) 42.25 cm^2 square and b) 314 cm^2 circle (both with a thickness of 0.5 mm). Filter holders for the AgNP papers include: c) square unit and d) plastic sieve inserted into bucket.

FIGURE 1. Images of different shapes and sizes of the AgNP Domtar paper: a) 42.25 cm2 square and b) 314 cm2 circle (both with a thickness of 0.5 mm). Filter holders for the AgNP papers include: c) square unit and d) plastic sieve inserted into bucket.
245x246mm (72 x 72 DPI)

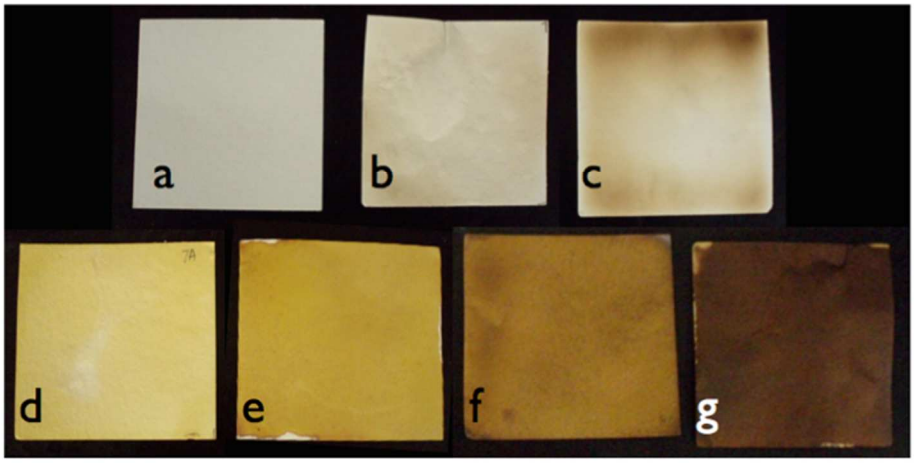

FIGURE 2. Domtar blotter papers without any silver (a) untreated, (b) heated in the microwave for 30 minutes, and (c) heated in the microwave for 6 minutes with glucose. Blotter papers were heated in the microwave for 4-6 minutes with 1M glucose and the following $AgNO_3$ concentrations: (d) 1 mM (e) 10 mM (f) 25 mM, and (g) 100 mM (each sheet is 6.5 x 6.5 cm) to form silver nanoparticles in the sheets.

FIGURE 2. Domtar blotter papers without any silver (a) untreated, (b) heated in the microwave for 30 minutes, and (c) heated in the microwave for 6 minutes with glucose. Blotter papers were heated in the microwave for 4-6 minutes with 1M glucose and the following AgNO3 concentrations: (d) 1 mM (e) 10 mM (f) 25 mM, and (g) 100 mM (each sheet is 6.5 x 6.5 cm) to form silver nanoparticles in the sheets.

268x197mm (72 x 72 DPI)

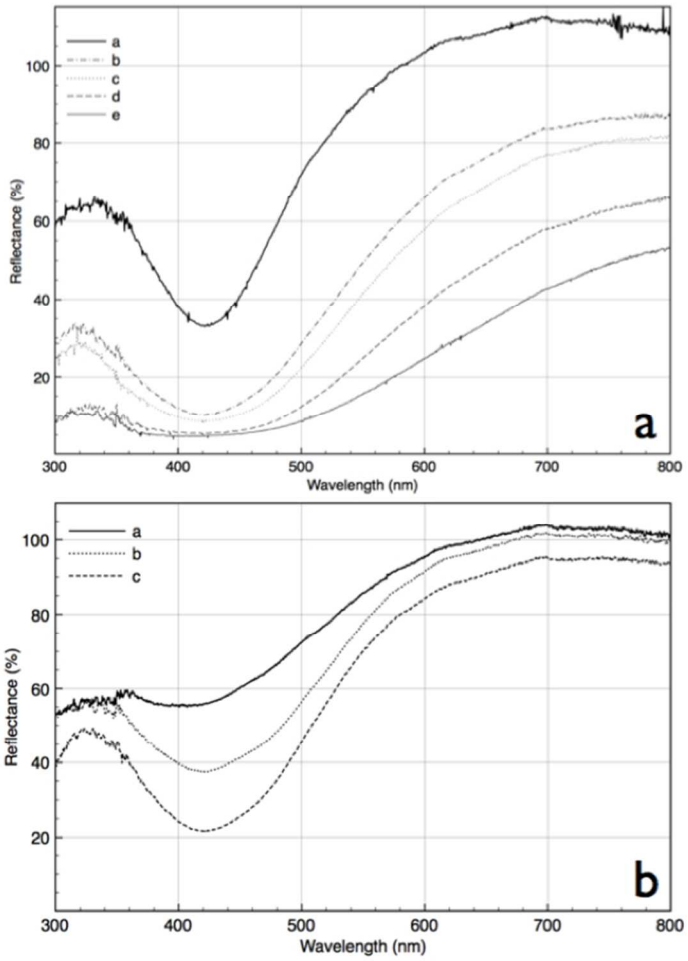

FIGURE 3a. UV-Visible reflectance spectra of paper sheets after being soaked with 1M glucose and increasing silver nitrate concentrations: a) 1 mM, b) 5 mM, c) 10 mM, d) 25 mM, and e) 50 mM, and then heated by microwave irradiation. 3b. UV-Visible reflectance spectra of paper sheets with different initial glucose concentrations: a) 0.01 M b) 0.1M and c) 1.0 M, and 1 mM $AgNO_3$ as the initial silver ion concentration, prepared by oven heating at 105°C for 70 minutes.

FIGURE 3a. UV-Visible reflectance spectra of paper sheets after being soaked with 1M glucose and increasing silver nitrate concentrations: a) 1 mM, b) 5 mM, c) 10 mM, d) 25 mM, and e) 50 mM, and then heated by microwave irradiation. 3b. UV-Visible reflectance spectra of paper sheets with different initial glucose concentrations: a) 0.01 M b) 0.1M and c) 1.0 M, and 1 mM AgNO3 as the initial silver ion concentration, prepared by oven heating at 105°C for 70 minutes.
270x361mm (72 x 72 DPI)

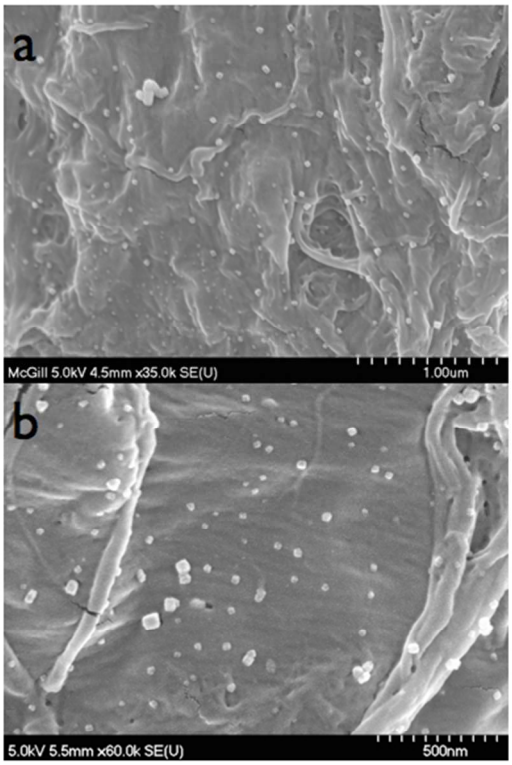

FIGURE 4. Scanning electron microscope image of AgNP paper with 2.5 mg Ag/ g paper, formed by heating in microwave oven: (a) 35,000 x and (b) 60,000 x magnification.

FIGURE 4. Scanning electron microscope image of AgNP paper with 2.5 mg Ag/ g paper, formed by heating in microwave oven: (a) 35,000 x and (b) 60,000 x magnification.
268x270mm (72 x 72 DPI)

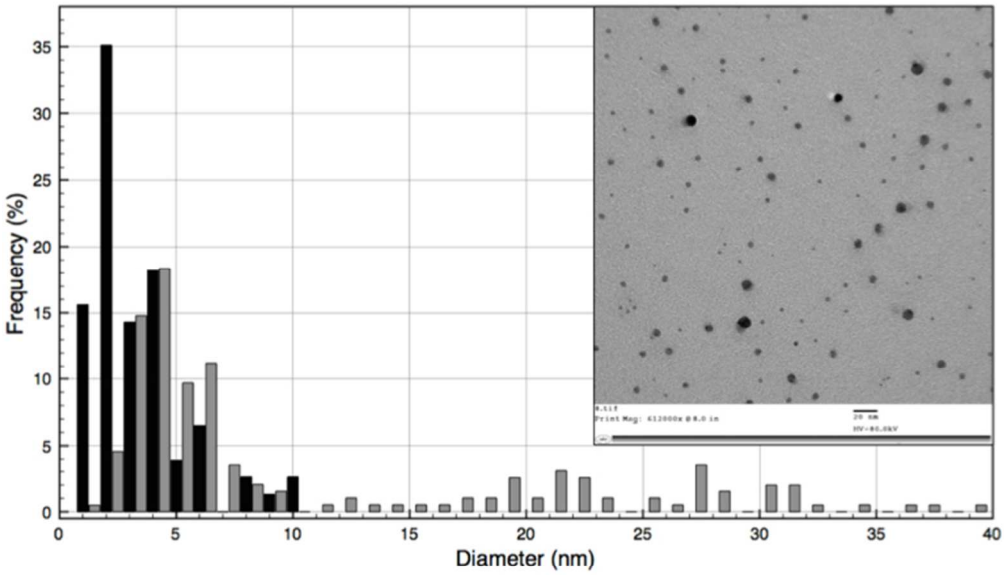

FIGURE 5. Nanoparticle diameter size histogram of silver nanoparticles in blotting paper with 1M glucose concentration (black bars) and no glucose (gray bars), and heated in the microwave. Inset of TEM image of silver nanoparticles formed with glucose reduction and microwave irradiation.

FIGURE 5. Nanoparticle diameter size histogram of silver nanoparticles in blotting paper with 1M glucose concentration (black bars) and no glucose (gray bars), and heated in the microwave. Inset of TEM image of silver nanoparticles formed with glucose reduction and microwave irradiation.
269x214mm (72 x 72 DPI)

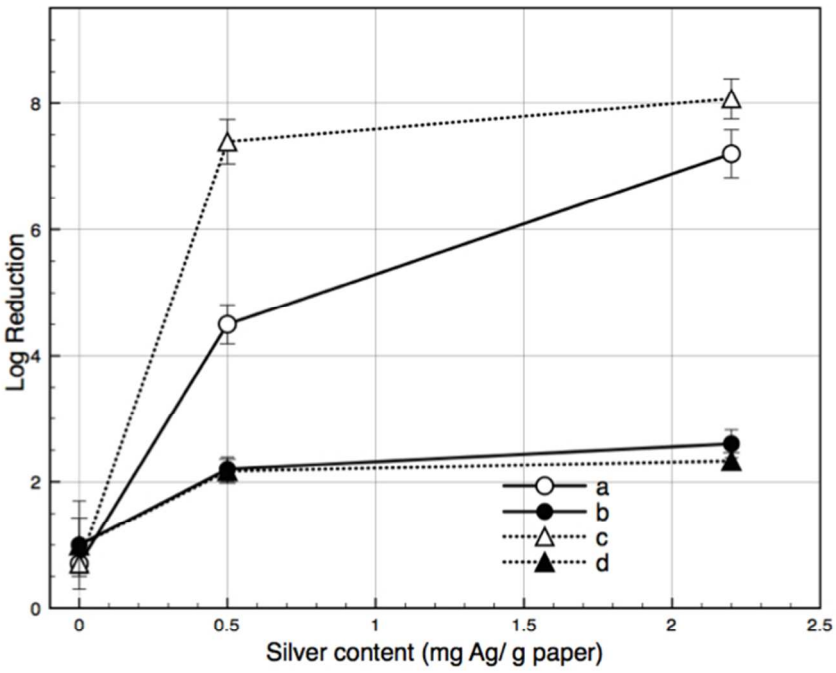

FIGURE 6. Log reduction of *E. coli* (a), (c), and *E. faecalis* (b), (d), bacterial count after permeation through the silver nanoparticle paper, at different silver contents in paper. (a) and (b) represent AgNP papers formed via sodium borohydride reduction. (c) and (d) represent AgNP papers formed via glucose and heat reduction via both microwave and conventional oven. (There was no significant differences between heating methods, so the results are averaged.) Initial bacterial concentration, $1x10^9$ CFU/mL for *E. coli* and $2x10^8$ CFU/mL for *E. faecalis*. Error bars represent standard error.

FIGURE 6. Log reduction of E. coli (a), (c), and E. faecalis (b), (d), bacterial count after permeation through the silver nanoparticle paper, at different silver contents in paper. (a) and (b) represent AgNP papers formed via sodium borohydride reduction. (c) and (d) represent AgNP papers formed via glucose and heat reduction via both microwave and conventional oven. (There was no significant differences between heating methods, so the results are averaged.) Initial bacterial concentration, 1E9 CFU/mL for E. coli and 2E8 CFU/mL for E. faecalis. Error bars represent standard error.
270x261mm (72 x 72 DPI)

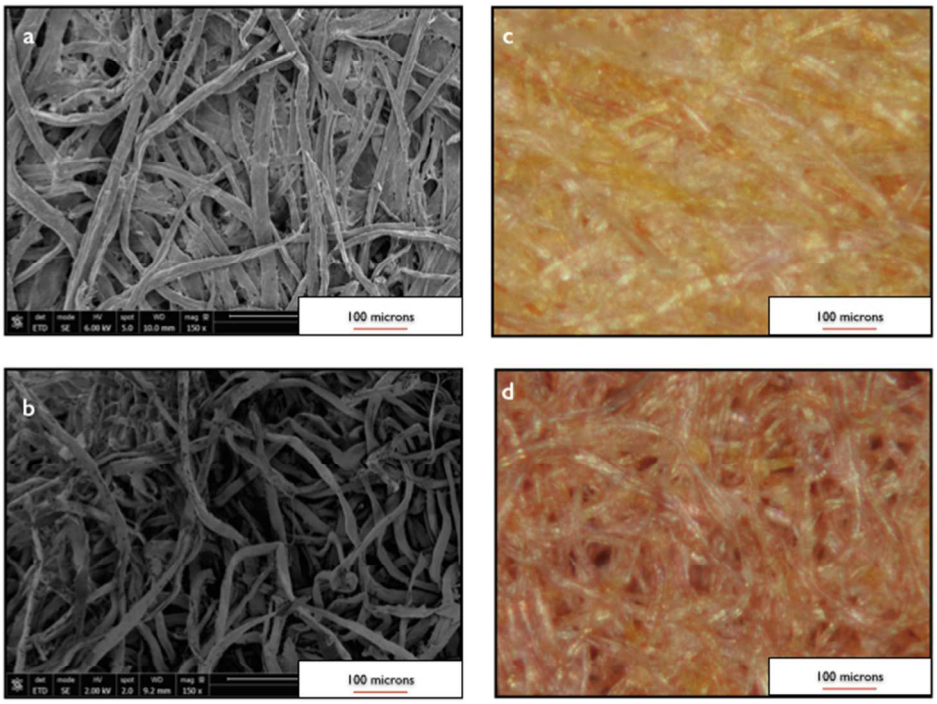

FIGURE 7. Scanning electron micrographs of the fiber packing density of the (a) Domtar and (b) GP Cellulose (732 g/m^2) papers. Dark field microscopy images of (c) Domtar and (d) GP Cellulose (732 g/m^2) papers. Magnification is 150 times.

FIGURE 7. Scanning electron micrographs of the fiber packing density of the (a) Domtar and (b) GP Cellulose (732 g/m2) papers. Dark field microscopy images of (c) Domtar and (d) GP Cellulose (732 g/m2) papers. Magnification is 150 times.
261x236mm (72 x 72 DPI)

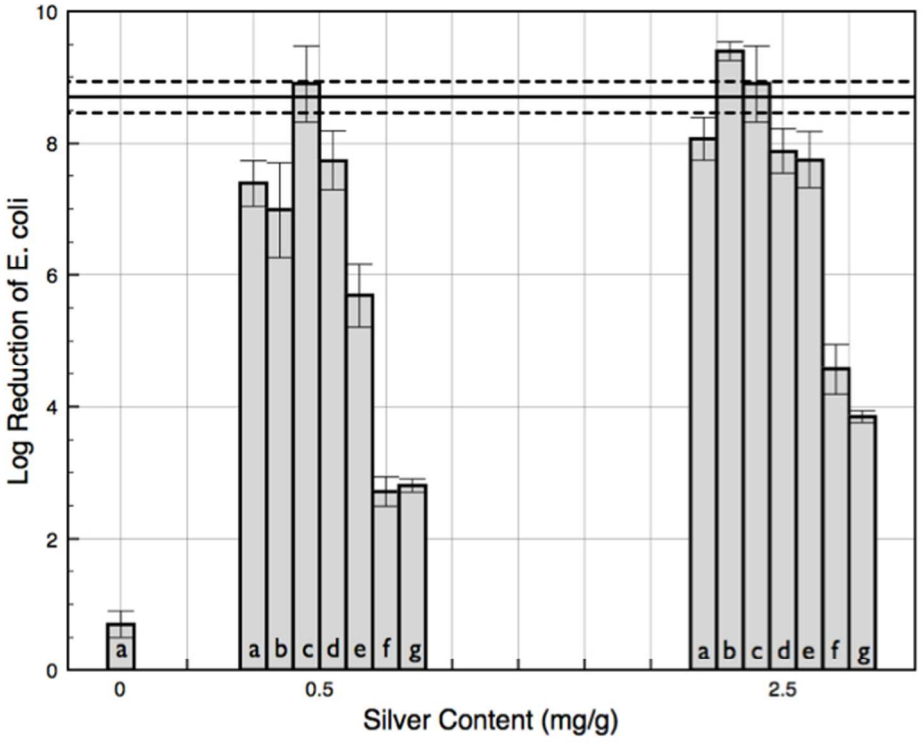

FIGURE 8. Log reduction of *E. coli* bacterial count after permeation through the silver nanoparticle paper, with different influent solutions: (a) deionized water, (b) 10 mg/L fulvic acid, (c) 50 mg/L fulvic acid, (d) phosphate buffered saline, (e) 2.5 g/L LB broth, (f) 25 g/L LB broth, and (g) 10 g/L tryptone. Initial bacterial concentration, $1x10^9$ CFU/mL for *E. coli*. Error bars represent standard error.

FIGURE 8. Log reduction of E. coli bacterial count after permeation through the silver nanoparticle paper, with different influent solutions: (a) deionized water, (b) 10 mg/L fulvic acid, (c) 50 mg/L fulvic acid, (d) phosphate buffered saline, (e) 2.5 g/L LB broth, (f) 25 g/L LB broth, and (g) 10 g/L tryptone. Initial bacterial concentration, 1x109 CFU/mL for E. coli. Error bars represent standard error.
267x261mm (72 x 72 DPI)